International Journal of Nanomedicine Dovepress

Open Access Full Text Article ORIGINAL RESEARCH

Naked Gene Delivery Induces Autophagy for Effective Treatment of Acute Lung Injury in a Mouse Model

Yu-Yan Qin[1,*], Hui Yu[1,2,*], Yong Huang[1,*], Xiaoyi Yang[1], Songpei Li[1], Ao Shen[1], Yinshan Lin[1], Mei Zhang[1], Qiulian Zhu[1], Jingwei Zhang[1], Lingmin Zhang[1], Xi-Yong Yu[1]

[1]Key Laboratory of Molecular Target & Clinical Pharmacology and the State & NMPA Key Laboratory of Respiratory Disease, School of Pharmaceutical Sciences & the Fifth Affiliated Hospital, Guangzhou Medical University, Guangzhou, Guangdong, 511436, People's Republic of China; [2]Hutchison Whampoa Guangzhou Baiyunshan Chinese Medicine Co., Ltd, Guangzhou, Guangdong, 510515, People's Republic of China

*These authors contributed equally to this work

Correspondence: Xi-Yong Yu; Lingmin Zhang, School of Pharmaceutical Sciences, Guangzhou Medical University, Xinzao Road, Panyu District, Guangzhou, 511436, People's Republic of China, Email yuxycn@gzhmu.edu.cn; zhanglm@gzhmu.edu.cn

Background: Acute lung injury (ALI) leads to diffuse pulmonary interstitial and alveolar edema, further developing into acute respiratory distress syndrome (ARDS). The present therapeutic approaches showed limited effects with poor clinical efficacy or severe side effects. This study aims to develop novel pharmaceutical agents to reduce lung damage with acceptable side effects for ALI.

Methods: Naked gene delivery system based on epigallocatechin 3-gallate (EGCG) was synthesized to deliver plasmid expressing DNA damage regulated autophagy modulator 1 (DRAM1), designated as EGCG/DRAM1 (ED). ED was characterized by dynamic light scattering analysis and transmission electron microscope. The biodistribution of ED in mice was measured by an in vivo small animal imaging system. The therapeutic potentials of ED were evaluated in MLE12 cells and LPS-induced ALI mice.

Results: Our results showed that ED was nearly spherical with a diameter of ~100 nm and increased the stability of DRAM1 plasmid that encapsulated. The synthesized ED showed negligible toxicity at the selected experimental concentration in MLE12 cells. ED could be taken up by MLE12 cells with high efficiency and escape from the lysosome. In ALI mice, ED facilitated the accumulation and retention of DRAM1 plasmid in lung, and attenuated pulmonary edema and pulmonary vascular permeability. The therapeutic effects of ED on ALI were associated with increased autophagy and reduced oxidative stress in lung.

Conclusion: In summary, ED attenuated pulmonary edema and pulmonary vascular permeability, and improved pulmonary dysfunction in ALI mice. This naked gene delivery system for autophagy enhancement may serve as a potential therapeutic strategy to attenuate ALI.

Keywords: acute lung injury, EGCG, DRAM1, autophagy, oxidative stress

Introduction

Acute lung injury (ALI) is the injury of alveolar epithelial cells and capillary endothelial cells caused by severe infection, trauma, shock, or inhalation of harmful gases. It is associated with diffuse pulmonary interstitial and alveolar edema that caused by severe inflammation and oxidative stress, and further develops into acute respiratory distress syndrome (ARDS).[1,2] Although glucocorticosteroids are widely used for the treatment of ARDS in the clinical setting, there is no consensus on their efficacy and safety.[3] Other inhaled antiasthmatics such as activated protein C, salbutamol and surfactants have been discontinued due to poor clinical efficacy or high side effects. Therefore, it is of great significance to develop novel pharmaceutical agents to reduce lung damage with acceptable side effects for ALI.

In eukaryotic cells, autophagy is a process in which misfolded proteins or damaged organelles are wrapped into vesicles, which fused with lysosomes to form autolysosomes and degraded the contents contained in them, so as to meet the metabolic needs of cells and renew some organelles.[4,5] Autophagy after tissue injury, as an adaptive response, is beneficial to maintain cell homeostasis by removing cell debris and damaged organelles. Studies have shown that

Received: 15 July 2024
Accepted: 17 October 2024
Published: 24 October 2024

Graphical Abstract

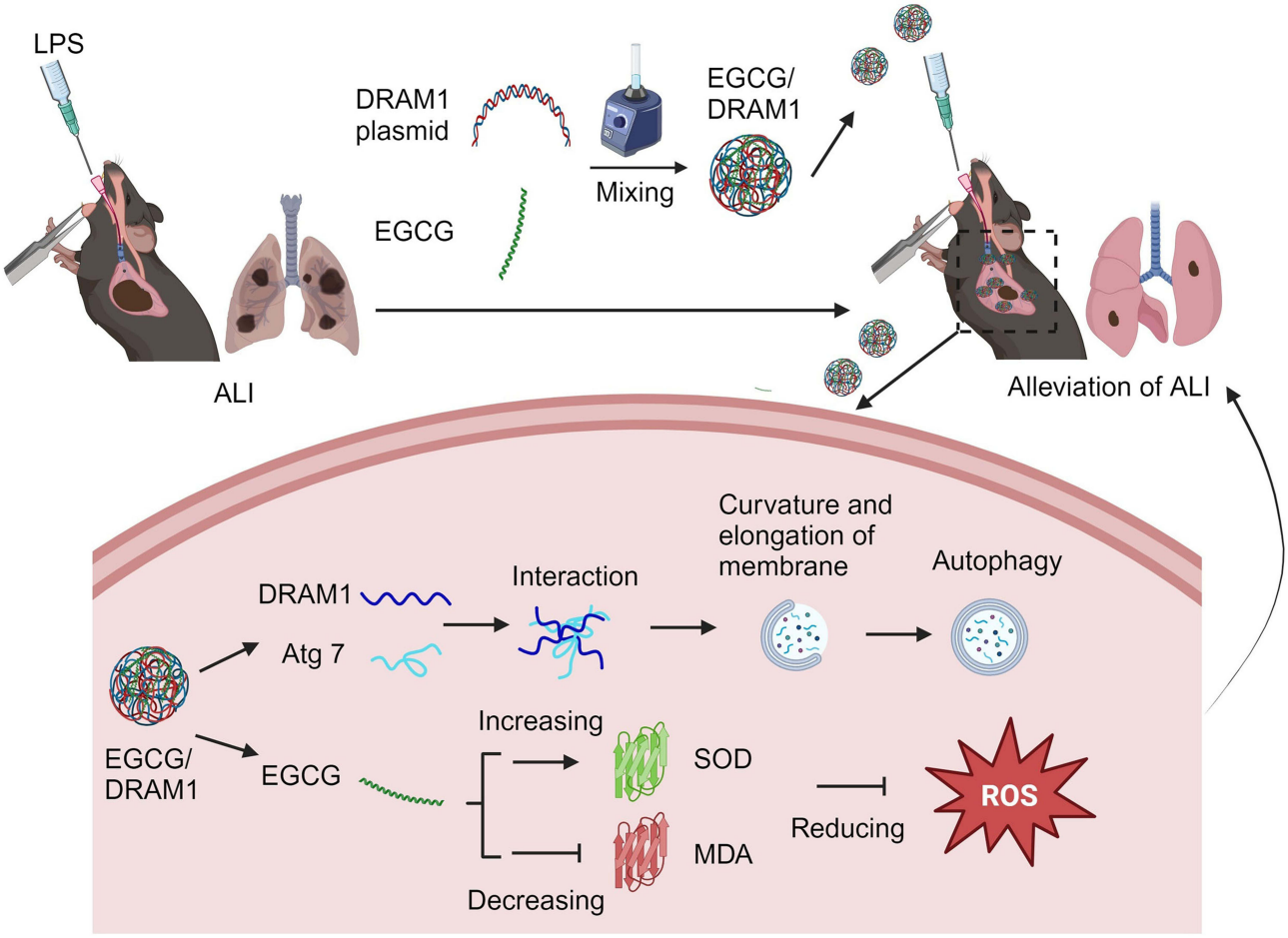

autophagy is involved in the pathogenesis of ALI.[6–8] Activation of autophagy played a protective role in ischemia/reperfusion (I/R)-induced lung injury in mice.[9] Fan et al found that promoting autophagy by proteasome inhibition protected rat alveolar macrophages from hypoxia-reoxygenation injury by suppressing endoplasmic reticulum stress.[10] Interestingly, inhibition of autophagy using 3-methyladenine aggravated A549 cells injury induced by lipopolysaccharide (LPS), while using 4-phenyl butyric acid to activate autophagy reduced LPS-induced inflammation and lung injury.[11] Therefore, targeting autophagy showed promise in the treatment of ALI.

DRAM1 (DNA damage regulated autophagy modulator 1) is a downstream target of p53 that induces autophagy to regulate apoptosis in response to cellular stresses.[12] Recently, it has been reported that DRAM1 promoted the fusion of lysosomes with autophagosomes to facilitate the degradation of autophagic body, thereby regulating autophagy flux.[13–15] Our recent work also found that DRAM1 interacted with Atg7, accompanied by increased Atg12-Atg5 conjugation, which promoted the bending and elongation of autophagosomes, accelerating autophagy flux and thereby reversing post-myocardial infarction heart remodeling.[16]

Epigallocatechin 3-gallate (EGCG) is a major active ingredient of green tea with anti-inflammatory, antioxidant, and anti-cancer effects.[17,18] It has been shown that pulmonary targeted delivery of EGCG significantly suppressed inflammatory and the growth of mycobacterium tuberculosis by enhancing the autophagy.[19] The anti-tumor effect of EGCG is partially mediated by the activation of autophagy in tumor cells.[20] Autophagy enhanced by EGCG protected human aortic endothelial cells from oxidative stress-induced apoptosis.[21] Despite diverse bioactivities, EGCG has poor bioavailability with a short half-life (3.4 ± 0.3 h), which hampers its further development for clinical application.[18,22] Previous

reports indicated that EGCG could assemble with nucleic acids or proteins into stable nanocomplexes via the formation of hydrogen bonds.[23–25]

In this study, we reported a strategy to fabricate nanoparticles for plasmid delivery. The nanoparticle consists of EGCG and plasmid encoding DRAM1 (EGCG/DRAM1). EGCG forms numerous hydrogen bonds and hydrophobic interactions with the DRAM1-expressing plasmid via hydroxyl-rich moieties, eventually becoming a stable nanocomplex. We hypothesized that EGCG/DRAM1 integrated the enhancement of autophagy induced by overexpressing DRAM1 and the antioxidative effects of EGCG to treat ALI. The EGCG/DRAM1 increased the expression of DRAM1 protein, which interacted with Atg7 and promoted the bending and elongation of autophagosomes to accelerate autophagy flux, thus reversing ALI. In addition, EGCG/DRAM1 increased the activity of superoxide dismutase (SOD) and decreased malondialdehyde (MDA) levels in ALI mice.

Material and Methods

The Synthesis of EGCG/DRAM1 Nanoparticles

EGCG (Lot#SLCK1721) and LPS (Lot#057M4013V) were obtained from Sigma-Aldrich. An expression cassette containing mouse DRAM1 (accession number NM_027878.3) and EYFP coding sequence was synthesized by Tsingke Biotechnology (Beijing, China) and cloned into pcDNA3(+) vector, so that DRAM1 was fused with EYFP by a GGSGG linker.

EGCG was dissolved in PBS with a pH of 7.4, which was then mixed with DRAM1 plasmid. The ratio of EGCG was further optimized to formulate the nanoparticles ([EGCG]/[DRAM1 plasmid]) = 10/1, 20/1, 30/1, 40/1, 50/1, 60/1, 70/1, 80/1, 90/1, and 100/1). The mixtures were vortexed violently and allowed to rest for 30 min at room temperature. The formulated nanoparticles were named ED, which was collected by centrifugation at a speed of 20,000 × *g* at 4 °C. EGCG/DRAM1 plasmid = 50/1 was used in the following study. The EGCG/Null plasmid (EN) was prepared with null plasmid as a negative control.

Characterization of ED

ALI mice treated with 40 mg/kg EGCG showed the least Evans blue (EB) in the lungs compared to the mice treated with 0, 10, 20 and 60 mg/kg EGCG (Supplement Figure 1C and D). Therefore, EGCG/DRAM1 nanoparticle was prepared by 40 mg/kg EGCG and 3 μg/mL DRAM1 plasmid (Supplement Figure 2). A Nano ZS (Malvern, UK) was used to analyze the size, polydispersity index (PDI) and zeta potential. The morphologies of EGCG/DRAM1 nanoparticles were characterized by a transmission electron microscope (TEM, JEOL JEM-2100Plus 200 kV, Japan) at 100 kV and the RADIUS Software (EMSIS GmbH, Germany) was used to acquire images.

Agarose Gel Electrophoretic Mobility Shift Assay

The formation and stability of EGCG/DRAM1 nanoparticles were tested by electrophoretic mobility shift assay. DRAM1 plasmid or EGCG/DRAM1 nanoparticle (weight ratio 50/1) was separated by agarose gel electrophoresis at 80 V for 40 min after the incubation with serum for 1, 2, 3, 4 h. The images of gel were taken using the Amersham Imager 600 system (GE Healthcare Life Sciences, USA).

Cell Culture

Murine Lung Epithelial 12 (MLE12) was purchased from the Cell Resources Center of Shanghai Institutes for Biological Sciences, Chinese Academy of Sciences (SIBS, CAS, China). MLE12 cells were cultured in Dulbecco's modified Eagle's medium (DMEM, Cat#D5030, Sigma-Aldrich, St. Louis, MO) supplemented with 10% fetal bovine serum (Gibco, USA), 1% penicillin–streptomycin solution at 37°C in humidified incubators with a 5% CO_2 atmosphere. To determine whether EGCG/DRAM1 nanoparticles enhances autophagy flux, MLE12 cells were treated with EGCG/DRAM1 nanoparticles for 12 h before a stimulation with LPS (100 ng/mL) for 24 h and expression of LC3 II and LC3 I was detected by Western blot.

Cellular Uptake of EGCG/DRAM1 Nanoparticles in vitro

The cellular uptake of EGCG/DRAM1 nanoparticles by MLE12 cells was measured by confocal laser scanning microscopy (CLSM) and flow cytometry (FCM). MLE12 cells were seeded either in confocal dishes or in 6-well plates (5×10^5 cells/well). After cultured overnight, cells were incubated with Cy5-labeled ED or Cy5-labeled DRAM1 plasmids (plasmids equivalent to 0.5–3.0 μg/mL) for 6 h, respectively. Cells in the confocal dishes were stained with actin-tracker green (Beyotime, China) and Hoechst 33342 (Beyotime, China) for CLSM analysis (Zeiss 880, Germany). Cells in the 6-well plates were digested by 0.25% EDTA-Trypsin and prepared in single cell suspension for FCM analysis (Merck, USA) to quantify the amount of Cy5 positive cells.

Furthermore, evaluation of the cellular uptake of EGCG/DRAM1 nanoparticles over time was performed. MLE12 cells in confocal dishes or 6-well plates were incubated with EGCG/DRAM1 nanoparticles (Cy5-labeled plasmids equivalent to 3.0 μg/mL) for different durations (1, 2, 4, 6 and 12 h). Cells were stained with actin-tracker green and DAPI for CLSM analysis. Cells in the 6-well plates were prepared in single cell suspension and quantified by FCM analysis.

Lysosome Escape

MLE12 cells were seeded in confocal dishes at the intensity of 5×10^5/mL and incubated for 12 h prior to the following experiments. Cy5-labeled EGCG/DRAM1 nanoparticles containing 3.0 μg/mL plasmid was incubated with cells for 3 or 9 h. Cells were washed by 1 × PBS for 3 times and stained with a Lysotracker (Thermo, USA) for 15 min. The images were taken by using a CLSM (Zeiss, Germany).

Transfection Efficiency

MLE12 cells were seeded either in confocal dishes or in 6-well plates at the intensity of 2×10^5/mL and incubated for 12 h prior to the following experiments. EGCG/DRAM1 nanoparticles (plasmids equivalent to 0–3.0 μg/mL) was incubated with cells for 12 h. Cells were washed with 1 × PBS for 3 times and cultured in fresh medium for another 36 h. Cells were imaged by CLSM (Zeiss, Germany) or analyzed by FCM (Merck, USA) to detect the intensity of YFP.

Cytotoxicity in vitro

The cytotoxicity of nanoparticles in vitro was evaluated by Live/Dead staining and apoptotic assay. Briefly, MLE12 cells at a density of 2×10^5/mL were seeded into confocal dishes or 6-well plates and cultured overnight. Cells were incubated with multiple concentrations of EGCG (0, 6.25, 12.5, 25, 50, 100 and 200 μg/mL), DRAM1 plasmid (0, 0.0625, 0.125, 0.25, 0.5, 1 and 2 μg/mL) or EGCG/DRAM1 nanoparticles (0, 6.25, 12.5, 25, 50, 100 and 200 μg/mL) for 12 h and cultured in fresh medium for another 36 h. Cells were stained with Calcein-AM and PI (Beyotime, China) for 15 min, and live and dead cells were imaged by CLSM. Annexin V-FITC/PI was used to stain transfected MLE12 cells for FCM analysis. Cells were treated with 75% Ethanol as a positive control.

Animal Model of ALI

Animal studies were performed according to the Guide for the Care and Use of Laboratory Animals published by US National Institutes of Health (NIH publication no. 85–23, revised, 1996). The animal studies were approved by Experimental Animal Ethics Committee of Guangzhou Medical University (No. G2022-372). The C57BL/6J male mice at 8 weeks of age (body weight around 20–22 g) were acquired from Vital River Laboratory Animal Center (Beijing, China). As previously mentioned, LPS was administered by the trachea to establish a mouse model of ALI.[26,27] Mice treated with 5 mg/kg LPS showed the most EB content in the lungs compared to the mice treated with 1 and 2.5 mg/kg LPS (Supplement Figure 1A and B). Therefore, 5 mg/kg LPS was used to establish the model. Mice were anaesthetized by injecting 1% pentobarbital sodium intraperitoneally (50 mg/kg) and followed by 5 mg/kg LPS injection into the trachea with a microsyringe. After intratracheal instillation, the mice were kept vertical for 1 min to ensure the distribution of the LPS or saline in the lungs. Mice from different groups received tracheal administration of EGCG/DRAM1 nanoparticles, EGCG/Null nanoparticles, EGCG or DRAM1 plasmid once a day for 3 consecutive days.

Lung Function Assay

Lung function assay was performed as described previously.[28] Briefly, mice were anesthetized with 90 mg/kg pentobarbital sodium in order to inhibit the autonomous respiration. Then, the tracheas of mice were exposed and cut open to connect to the spirometer (Chest, Tokyo, Japan) with the frequency of 90. The respiratory quotient was 15:10 and the unit of the tidal volume was set as mL/kg. The scanner was monitored using a computer, and the lung function-related parameters were recorded, including airway resistance (Raw), pulmonary dynamic compliance (Cdyn), peak expiratory flow (PEF) and maximal mid-expiratory flow (MMF).

In vivo Imaging

1 × PBS, Cy5-labeled DRAM1 plasmid, and Cy5-labeled EGCG/DRAM1 nanoparticles were given to mice after the induction of ALI (n = 3). The fluorescence signals in the mice were monitored at time points of 3, 6, 12, 24, and 48 h using an imaging system (IVIS Lumina XRMS Series III, PerkinElmer, USA). The fluorescence signal of extracted heart, liver, spleen, lung and kidney were detected after 48 h, and the fluorescence intensity was quantified using Living Image (64-bit) software.

Lung Wet-to-Dry Weight Ratio

The mice were anesthetized and sacrificed after LPS-induced ALI on day 3. Right lung tissue was collected (n = 5) and surface blood was removed. The wet weight of the lungs was determined, then the lungs were dried at 60°C for 72 h to obtain the dry weight as previously mentioned.[29] The wet/dry weight ratio was calculated.

Vascular Permeability of Lung

The animals were injected with EB (50 mg/kg) through femoral vein 15 min before the animals were sacrificed (n = 5 per group). The lungs were removed after thoracotomy, and the surrounding tissues were cut off from the upper lobe of the right lung. The lungs were immersed in formamide solution (1 mL/100 mg animal weight) and incubated at 45–50°C for 72 h. After all the pigments in the tissues were leached, the tissues were removed and centrifuged. The supernatant was taken, and colorimetric measurement was performed at 620 nm by spectrophotometer. Optical density (OD) value of formamide solution was determined. EB content per gram of wet lung tissue was calculated according to the concentration corresponding to the standard curve.

Histological Evaluation

Changes in left lungs morphology (n = 5) were assessed in methyl Carnoy's fixed, paraffin-embedded tissue slices (4 μm) with hematoxylin and eosin (H&E) staining, according to the reported methods.[30,31] Images were captured using a microscope (Olympus Optical Co., Ltd., Tokyo, Japan). Severity of lung injury was evaluated and scored in a blinded manner based on four aspects: congestion of alveolar-capillary membrane, hemorrhage, infiltration or aggregation of neutrophils in the air space or the vessel wall, and thickness of the alveolar wall/hyaline membrane formation. Each of the four components was scored from 0 to 4, respectively, depending on the severity and summarized to generate a final score ranging from 0 to 16 as previously reported.[32,33]

Transmission Electron Microscopy

Fractions of the left lung tissues (n = 5) were pre-fixed in a solution of 2.5% glutaraldehyde and 1% osmium tetroxide, post-fixed in 1% OsO_4, dehydrated in an escalating sequence of alcohols, and embedded in epoxy resin, as reported before.[8,34] Uranyl acetate and lead citrate were used to stain ultrathin sections. A transmission electron microscope (HITACHI H-600, Japan) was used to detect the autophagosome and autolysosome of samples.

Western Blot

The protein of lung tissues (n = 6) was extracted using RIPA lysis buffer, and Western blot analysis was performed as reported previously.[30,35] After blocking with 5% skim milk, membranes were incubated overnight at 4°C with 1:1000

dilutions of rabbit anti-DRAM1 (PRS4035, Sigma, USA), and rabbit anti-LC3 (Cat#3868, Cell Signaling Technology, USA), and GAPDH (ENZ-986, Chemicon) antibodies. Membranes were incubated with goat anti-rabbit (1:5000 dilution; Cat# ZB-2301, Beijing Zhong Shan - Golden Bridge Biological Technology, China) secondary antibody for 1 h at room temperature the next day after being washed with 1 × TBST 5 min for 3 times. Signals were scanned and visualized by an Amersham Imager 600 (GE, USA). The relative expression levels of proteins against GAPDH were quantified by using Image J software.

Immunoprecipitation

The MLE12 cells were lysed with immunoprecipitation buffer on ice for 30 min and centrifuged at 12,000 × *g* for 15 min at 4°C. The whole-cell lysates (500 μg) were incubated with 15 μL of protein agarose A/G beads to reduce nonspecific combination, followed by transient centrifugation to collect the supernatants. The supernatants were incubated with 15 μL of mouse IgG, rabbit IgG, or test antibodies mouse anti-Atg7 antibody (sc-376212, Santa Cruz Biotechnology, USA), at 4°C. Protein agarose A/G beads (~20 μL) was added to the supernatants, and the mixture was incubated for 4 h at 4°C the next day. After centrifuging at 4°C, 12,000 × *g* for 30s, the supernatant was carefully removed without touching the beads. And then, the beads were extensively washed three times with immunoprecipitation buffer 1, 2 and 3. SDS loading buffer (~25 μL) was added to the beads, after which the mixture was boiled for 5 min at 100°C. The immunoprecipitants were resolved by 12% SDS-PAGE followed by Western blot assay with respective antibodies including anti-Atg7 and anti-DRAM1.[8]

Determination of Malondialdehyde (MDA) and Superoxide Dismutase (SOD)

The supernatant of lung tissues (n = 6) was extracted with saline and analyzed using MDA (ab118970, Abcam, USA) and SOD (ab65354, Abcam, USA) assay kits according to the manufacturer's instruction.[36]

Statistical Analysis

The results were presented as mean ± SD. GraphPad Prism 8.0 was used to conduct one-way ANOVA with a Newman–Keuls post-hoc test (GraphPad Software, USA).

Results

The Preparation and Physicochemical Characterization of EGCG/DRAM1 Nanoparticles

The formulation of EGCG/DRAM1 nanoparticles were optimized by adjusting the ratio of EGCG to DRAM1 plasmid, namely 10, 20, 30, 40, 50, 60, 70, 80, 90, and 100 w/w, respectively. The ratio of 50/1 showed the minimized sized of 99.33 ± 11.68 nm with a PDI of 0.13 ± 0.01 (Figure 1A). We also measured the average zeta potentials of EGCG/DRAM1 nanoparticles, as the weight ratio of EGCG/DRAM1 plasmid increase, the zeta potential increase form negative to positive. The zeta potential of optimized EGCG/DRAM1 nanoparticles (50/1) was 11.7 ± 1.06 mV (Figure 1B). We used this formulation to prepare EGCG/DRAM1 nanoparticles for the subsequent evaluations. TEM and dynamic light scattering (DLS) analysis indicated that EGCG/DRAM1 nanoparticle was nearly spherical with a diameter of ~100 nm (Figure 1C and D). Furthermore, the formation of EGCG/DRAM1 nanoparticles inhibited the degradation of DRAM1 plasmid in serum (Figure 1E). These results indicated that EGCG enabled to increase the stability of DRAM1 plasmid.

The Biological Effect of EGCG/DRAM1 Nanoparticles in vitro

The transfection efficiency was evaluated by CLSM and FCM. The fluorescence dye Cy5 was used to label EGCG/DRAM1 nanoparticles. After the cells were incubated with Cy5- EGCG/DRAM1 nanoparticles for 12 h, the fluorescence of Cy5 was used as a marker for evaluation of cellular uptake. CLSM and FCM analysis indicated that cells treated with Cy5- EGCG/DRAM1 nanoparticles containing 3.0 μg plasmid showed 96.4% of Cy5 positive cells, which was the highest percentage among the tested formulations (Figure 2A and B). Therefore, we chose Cy5- EGCG/DRAM1 nanoparticles containing 3.0 μg of DRAM1 plasmid for the following experiments.

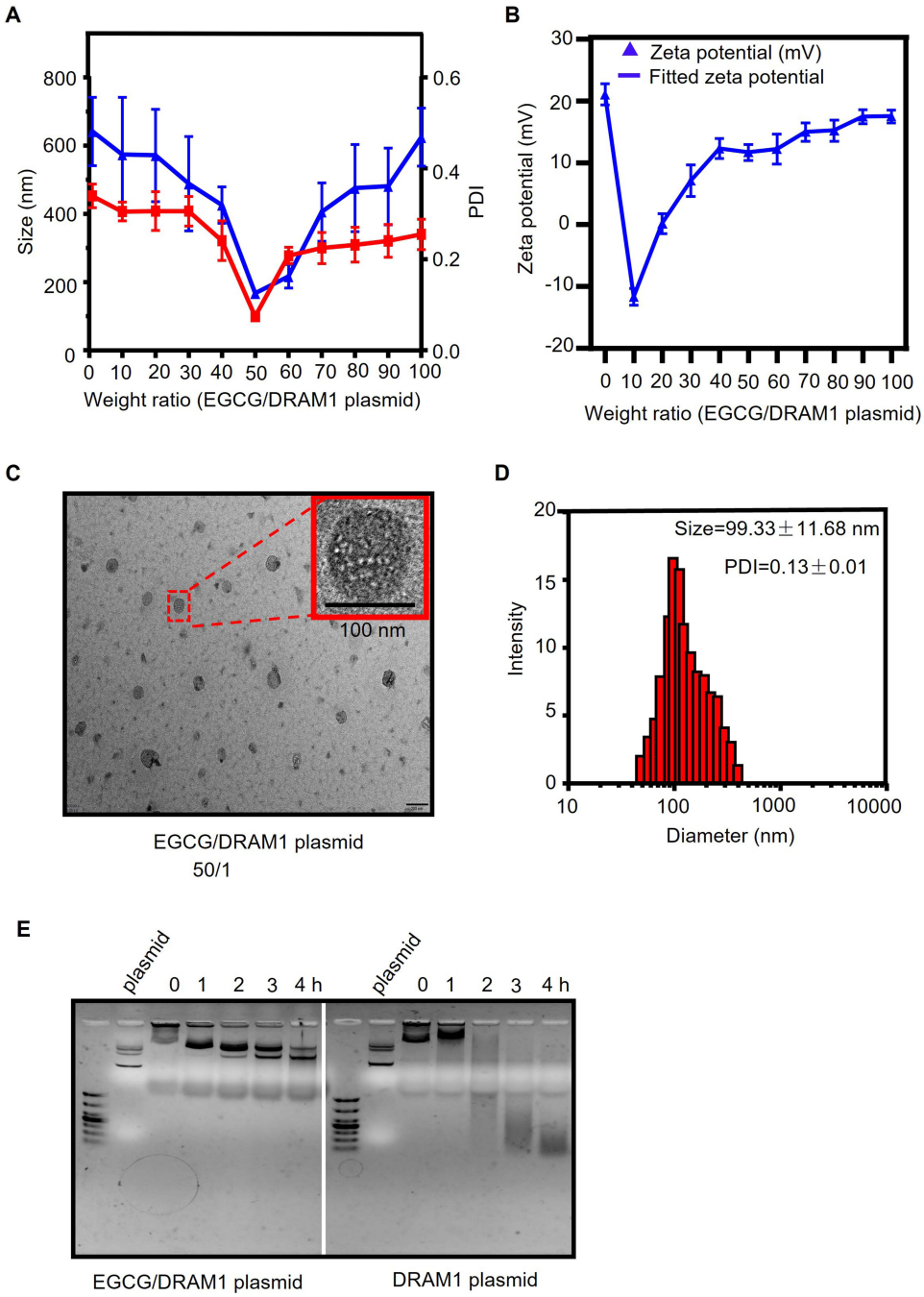

Figure 1 Characterization of EGCG/DRAM1 plasmid nanoparticles (ED). (**A**) Size and polydispersity index (PDI) of ED with multiple weight ratio by dynamic light scattering (DLS) analysis. (**B**) Zeta potential of ED with multiple weight ratio by DLS analysis. (**C**) Transmission electron microscope (TEM) image of EGCG/DRAM1 plasmid weight ratio of 50/1. (**D**) Size and PDI of ED at an EGCG/DRAM1 plasmid weight ratio of 50/1 by DLS analysis. (**E**) Agarose gel electrophoretic mobility shift assay of ED and naked DRAM1 plasmid after the incubation with serum for 1, 2, 3, 4 h.

Furthermore, we found that the cellular uptake of EGCG/DRAM1 nanoparticles by MLE12 cells was time dependent. After the incubation with Cy5-EGCG/DRAM1 nanoparticles, the Cy5 fluorescence in cells gradually increased over time and 89.8% of cells were Cy5 positive at the time point of 6 h as indicated by CLSM and FCM (Figure 3). The transfection for 12 h led to a maximum cellular uptake (98.1% Cy5 positive cells) (Figure 3). Thus, the optimized condition for effective transfection by EGCG/DRAM1 nanoparticles was 12 h with a DRAM1 plasmid equivalent to 3.0 μg.

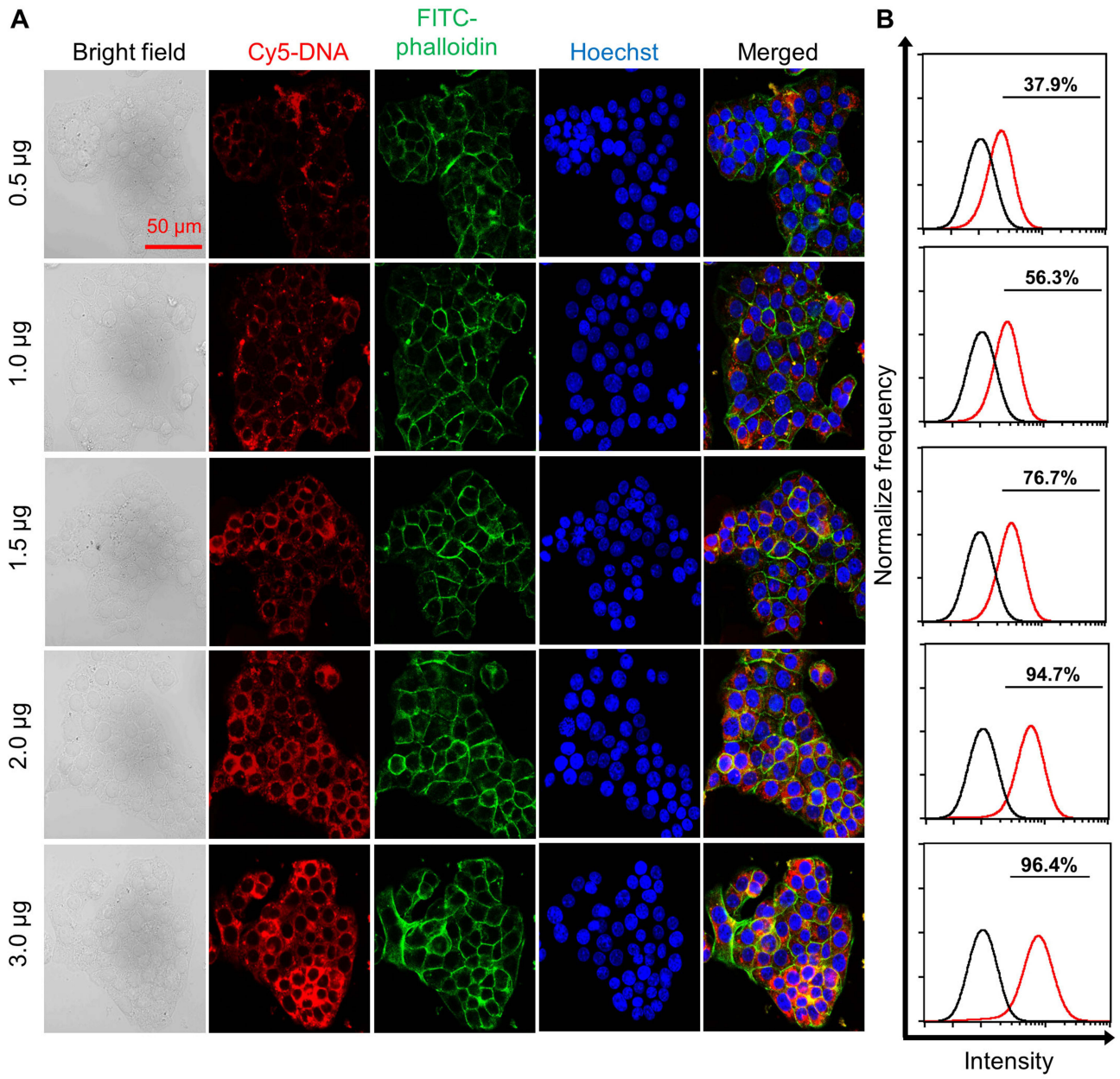

Figure 2 The transfection efficiency of ED. (**A**) Confocal laser scanning microscope (CLSM) of the transfection efficiency of ED at different concentrations. (**B**) Quantification of Cy5 positive cells by Flow Cytometry (FCM) analysis.

Cellular uptake is a prerequisite for efficient gene overexpression by plasmid and lysosome escape is also a key process that determines the transfection efficiency. CLSM analysis indicated that most of DRAM1 plasmid were captured by the lysosomes after an incubation for 3 h, as indicated by the overlap of green lysosome labeling by lysotracker and the red DRAM1 plasmid labeling by Cy5 (Figure 4). In contrast, the red fluorescence separated from the green signal at 9 h, indicating that the plasmid escaped from the lysosome. The data indicated that the plasmid in EGCG/DRAM1 nanoparticles was able to escape from the lysosome, which facilitated the subsequent expression of DRAM1 gene.

In addition, we evaluated the cytotoxicity of EGCG, DRAM1 plasmid and the synthesized EGCG/DRAM1 nanoparticles in MLE12 cells by using CCK8 assay, Calcein-AM/PI staining and annexin V-FITC/PI apoptotic assay. The EGCG, DRAM1 plasmid, and EGCG/DRAM1 nanoparticles did not significantly inhibit the cell viability at highest concentration that tested as indicated by CCK8 assay (Figure 5A-C). The results of Calcein-AM/PI staining also showed negligible PI positive cells and annexin V-FITC/PI assay showed less than 2% apoptotic cells after the treatment of

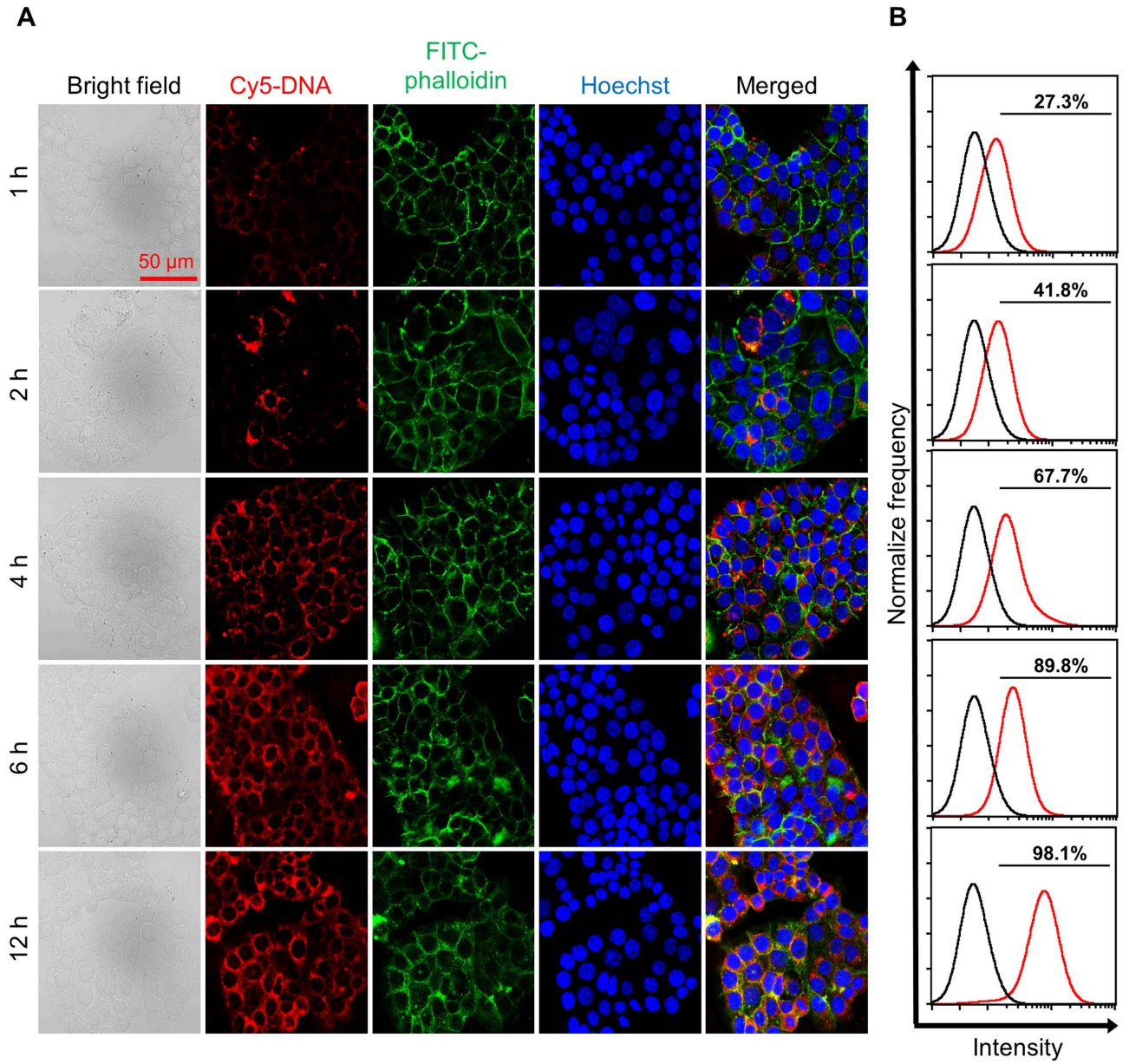

Figure 3 The time-dependence uptake of ED by MLE12 cells. (**A**) CLSM analysis of the transfection efficiency of ED for different incubation time. (**B**) Quantification of Cy5 positive cells by FCM analysis.

EGCG, DRAM1 plasmid and EGCG/DRAM1 nanoparticles, whereas ethanol as a positive control led to apparent apoptosis with 99.3% apoptotic cells (Figure 5D and 5E). Above data indicated that the cellular toxicity of the synthesized EGCG/DRAM1 nanoparticles was tolerable in MLE12 cells.

The Biodistribution of EGCG/DRAM1 Nanoparticles in vivo

Cy5-labeled plasmids were used to prepare EGCG/DRAM1 nanoparticles (Cy5- EGCG/DRAM1 nanoparticles) to evaluate the biodistribution of EGCG/DRAM1 nanoparticles in mice using an in vivo small animal imaging system. Cy5- EGCG/DRAM1 nanoparticles and Cy5-DRAM1 plasmid were injected via the trachea into ALI mice or sham group, respectively. The mice treated with EGCG/DRAM1 nanoparticles showed stronger fluorescence in the lung than sham or mice treated with DRAM1 plasmid at 3, 6, and 12 h (Figure 6A). Ex vivo imaging of the extracted organs also showed high level of fluorescence signals in lung after EGCG/DRAM1 nanoparticles treatment (Figure 6B).

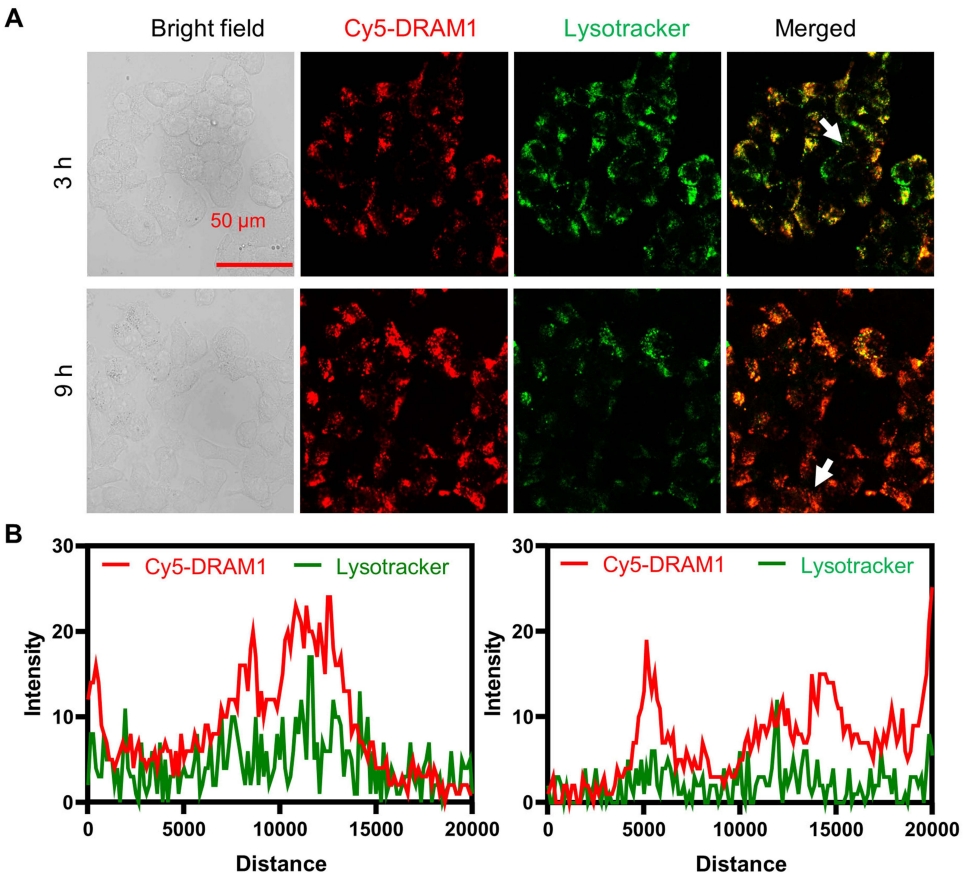

Figure 4 The lysosome escape of ED in MLE12 cells. (**A**) Detection of Cy5-DRAM1 and lysosome in MLE12 cells treated with ED for 3 h and 9 h. (**B**) The fluorescence intensity and distribution of (**A**).

Quantification of fluorescence intensity indicated that EGCG/DRAM1 nanoparticles induced a ~1.5-fold higher fluorescence in the lung compared with naked DRAM1 plasmid (Figure 6C). Above results suggested that the binding with ECGC facilitated the accumulation and retention of DRAM1 plasmid in the infected lungs.

The Attenuation of ALI by EGCG/DRAM1 Nanoparticles in Mice

In ALI mice, we investigated the therapeutic effects of EGCG/DRAM1 nanoparticles. The ALI mice were randomly assigned to six groups and given the following treatments via trachea: saline alone, EGCG alone, DRAM1 plasmid alone, EGCG/Null nanoparticles, and EGCG/DRAM1 nanoparticles. First, we measured the effect of EGCG/DRAM1 nanoparticles on lung function 3 days after ALI. ALI mice treated with saline developed severe lung dysfunction as evidenced by the increase of Raw (2.45 ± 0.31 cmH_2O mL/min vs 0.53 ± 0.22 cmH_2O mL/min), and the decreased of Cdyn (1.16 ± 0.34 mL/cmH_2O vs 2.63 ± 0.39 mL/cmH_2O), PEF (3.14 ± 0.33 mL/s vs 5.81 ± 0.54 mL/s) and MMF (2.18 ± 0.24 mL/s vs 3.10 ± 0.25 mL/s) compared with sham mice. ALI mice treated with EGCG, DRAM1 plasmid and EGCG/DRAM1 nanoparticles showed mild attenuation of lung dysfunction (Figure 7A). Of note, EGCG/DRAM1 nanoparticles showed the most potent effect on ameliorating lung dysfunction compared with other treatment groups as indicated by significantly decreased Raw to 1.16 ± 0.24 cmH_2O mL/min, and increased Cdyn to 2.08 ± 0.33 mL/cm H_2O, PEF to 5.08 ± 0.54 mL/s, MMF to 2.77 ± 0.16 mL/s. At the third day after ALI, mice were sacrificed and H&E staining showed interstitial edema, interalveolar septal thickening and intra alveolar and interstitial patchy hemorrhage in ALI mice. Only EGCG/DRAM1 nanoparticles treatment induced a significant reduction in the lung injury score compared with saline-treated ALI mice, although EGCG, DRAM1 and EGCG/Null nanoparticles led to a decreased trend (Figure 7B).

ALI leads to damage of alveolar epithelial cells and capillary endothelial cells, accompanied by severe inflammation and oxidative stress, resulting in diffuse pulmonary interstitial and alveolar edema.[1,2] The pulmonary edema was assessed using

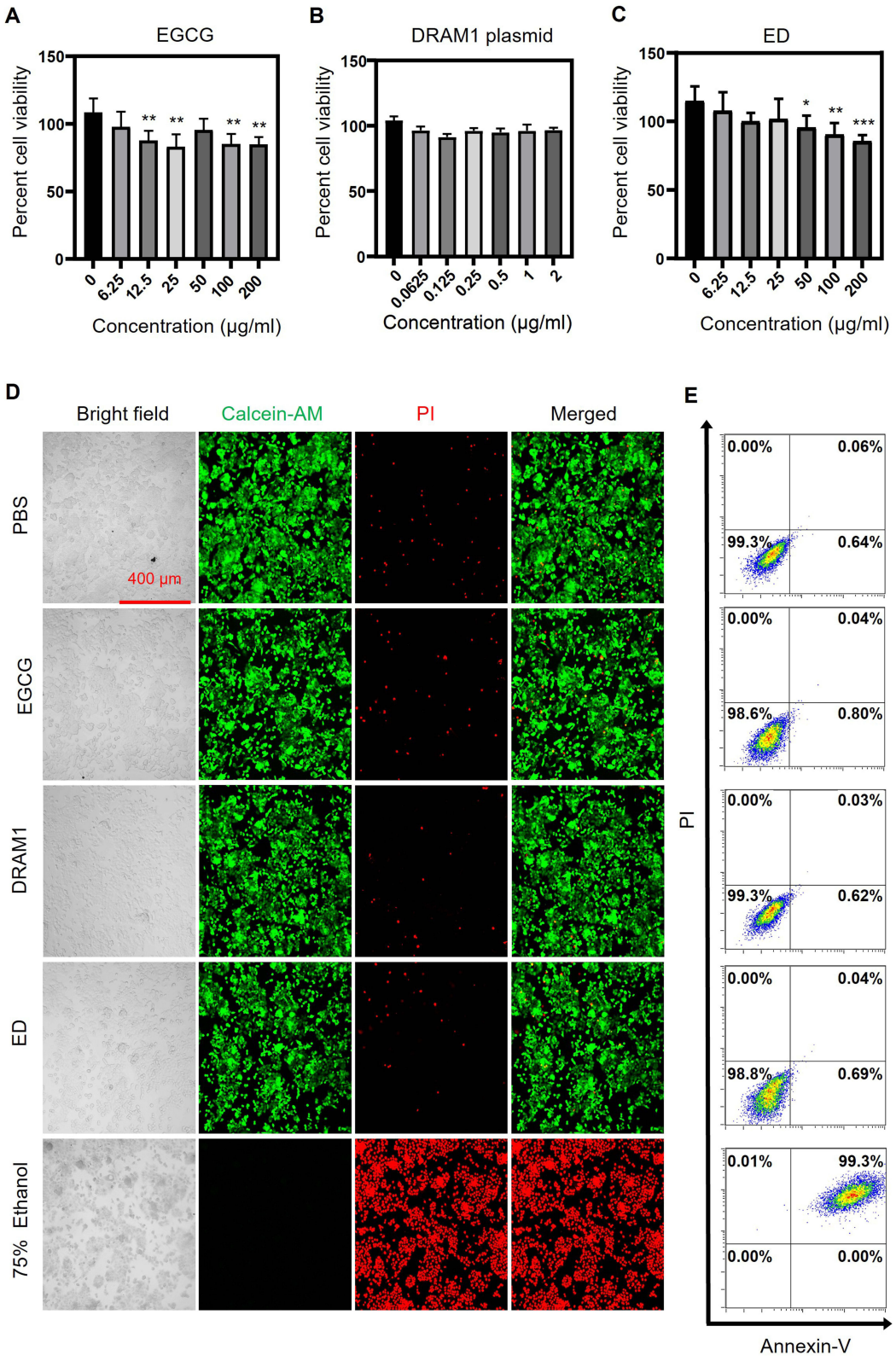

Figure 5 The cytotoxicity of EGCG, DRAM1 plasmid and ED to MLE12 cells. (**A-C**) The cell viability of MLE12 cells incubated with different concentration of EGCG, DRAM1 plasmid and ED by CCK8. Data were shown as mean ± SD for three independent experiments. **P*<0.05, ***P*<0.01, ****P*<0.001 vs 0 μg/mL group. (**D**) CLSM analysis of the live or dead MLE12 cells incubated EGCG, DRAM1 plasmid and ED after Calcein-AM/PI staining. (**E**) FCM analysis of apoptotic MLE12 cells incubated EGCG, DRAM1 plasmid and ED by annexin V-FITC/PI apoptotic assay.

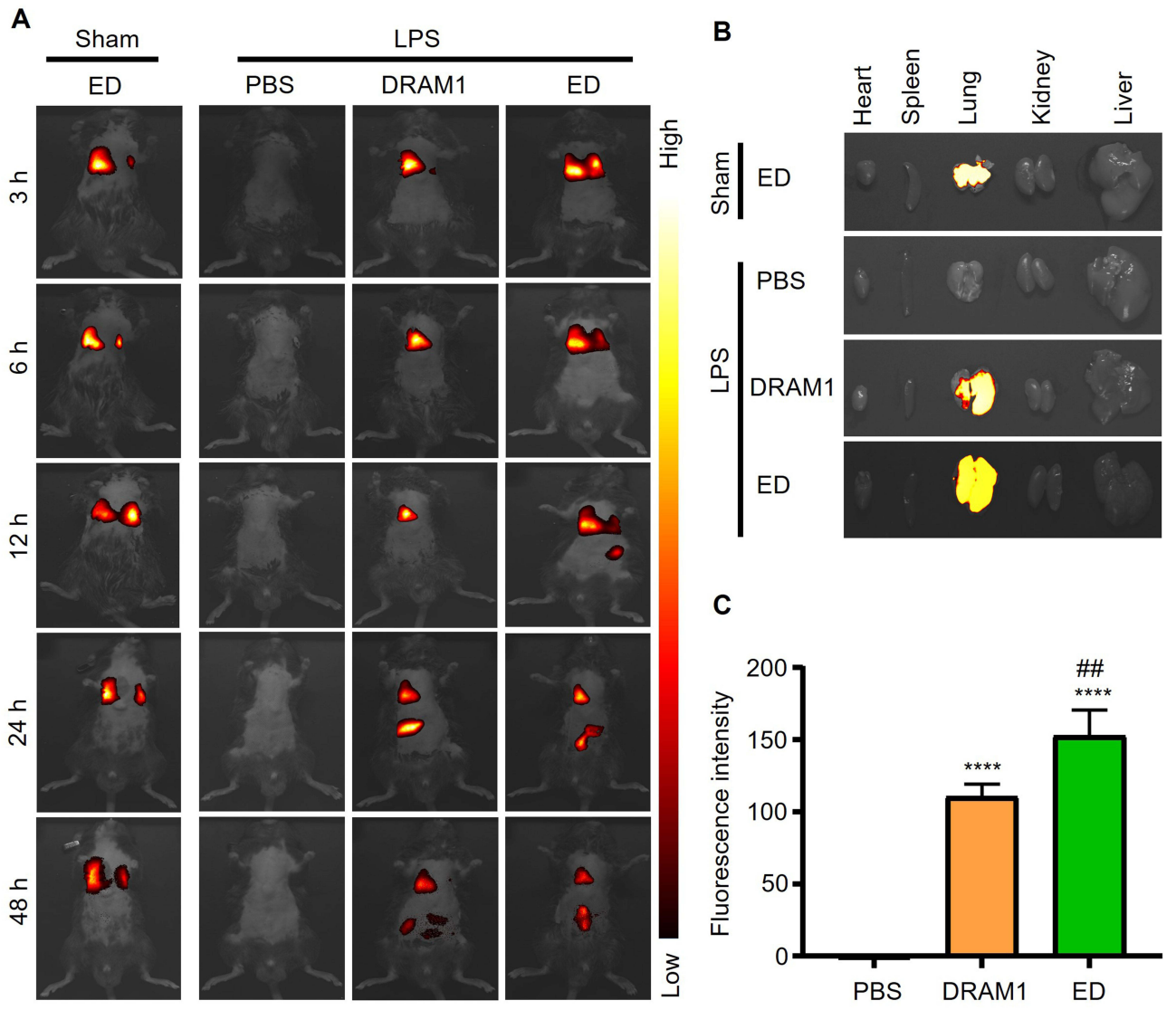

Figure 6 The biodistribution of ED in mice after ALI. (**A**) Detection of Cy5-plasmid signal after tracheal administration of ED or naked Cy5-DRAM1 plasmid at 3, 6, 12, 24, and 48 h by small animal in vivo imaging system (n = 3 per group). (**B**) Detection of the Cy5 signal in organs isolated from mice with tracheal administration of ED or naked Cy5-DRAM1 plasmid. (**C**) Relative Cy5 intensity in lung at 48 h. Data were shown as mean ± SD, n=3 mice per group. $^{****}P<0.0001$ vs PBS, $^{\#\#}P<0.01$ vs DRAM1.

wet-to-dry weight ratio (W/D) of lung and EB staining 3 days after ALI (Figure 8A-C). ALI mice treated with saline developed severe pulmonary edema with a W/D of ~8 and significantly increased microvascular permeability with an EB OD value of ~0.28. The EGCG, DRAM1 plasmid and EN mildly reduced pulmonary edema with less than 18% reductions in W/D (Figure 8C) and reduced microvascular permeability with an EB OD value of ~0.20 (Figure 8A and B). EGCG/DRAM1 nanoparticles most significantly decreased the W/D to ~5 and the EB OD value to ~0.15 (Figure 8B and C). Furthermore, the administration of the EGCG/DRAM1 nanoparticles decreased the expression of MDA, while increased the SOD activity in ALI mice as measured by test kit (Figure 8D and E).

The Mechanism Underlying the Effect of EGCG/DRAM1 Nanoparticles on Attenuating ALI

In order to further investigate the effect of EGCG/DRAM1 nanoparticles on autophagy in the microenvironment of lung injury, we used TEM and Western blot to analyze the autophagosome and autophagolysosome of the lung tissues 3 days after ALI. Compared to the treatment with saline, EGCG, DRAM1 plasmid or EGCG/Null nanoparticles, the mice treated with EGCG/DRAM1 nanoparticles showed significantly increased autophagy flux, which was demonstrated by

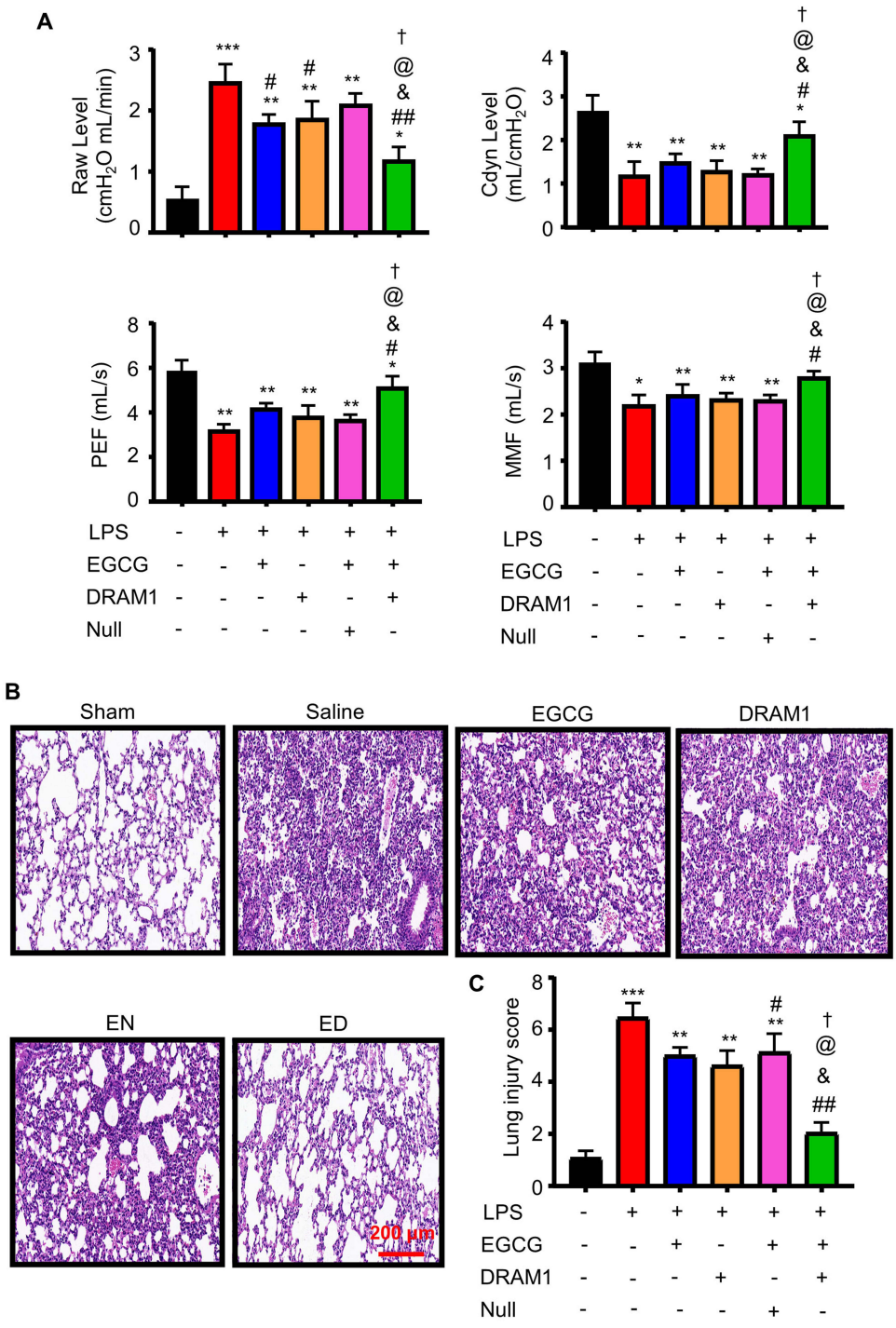

Figure 7 The effect of ED on lung function and lung injury. ALI mice were randomized into six groups and administered with the following treatments: saline, EGCG, DRAM1 plasmid, EN that fabricated with EGCG and null plasmid, and ED. (**A**) The lung function of different treatment groups that measured after tracheostomy, including pulmonary dynamic compliance (Cdyn), peak expiratory flow (PEF), and maximal mid-expiratory flow (MMF) and the airway resistance (Raw). (**B**) H&E staining of lung tissues from different treatment groups. (**C**) The lung injury scores of different treatment groups. Data were shown as mean ± SD, n=5 mice per group. $^{*}P < 0.05$, $^{**}P < 0.01$, $^{***}P < 0.001$ vs Sham, $^{\#}P < 0.05$, $^{\#\#}P < 0.01$ vs Saline, $^{\&}P < 0.05$ vs EGCG, $^{@}P < 0.05$ vs DRAM1, $^{\dagger}P < 0.05$ vs EN.

the elevation of autophagosome and autolysosome in the lung (Figure 9A) and increased LC3 II protein level (Figure 9B and C). These observations were also confirmed in MLE12 cells in which treated with EGCG/DRAM1 nanoparticles showed increased LC3 II protein level compared to PBS, EGCG, DRAM1 plasmid or EGCG/Null nanoparticles group (Figure 9D and E). DRAM1 interacts with Atg7 to promote the bending and elongation of autophagosomes and the

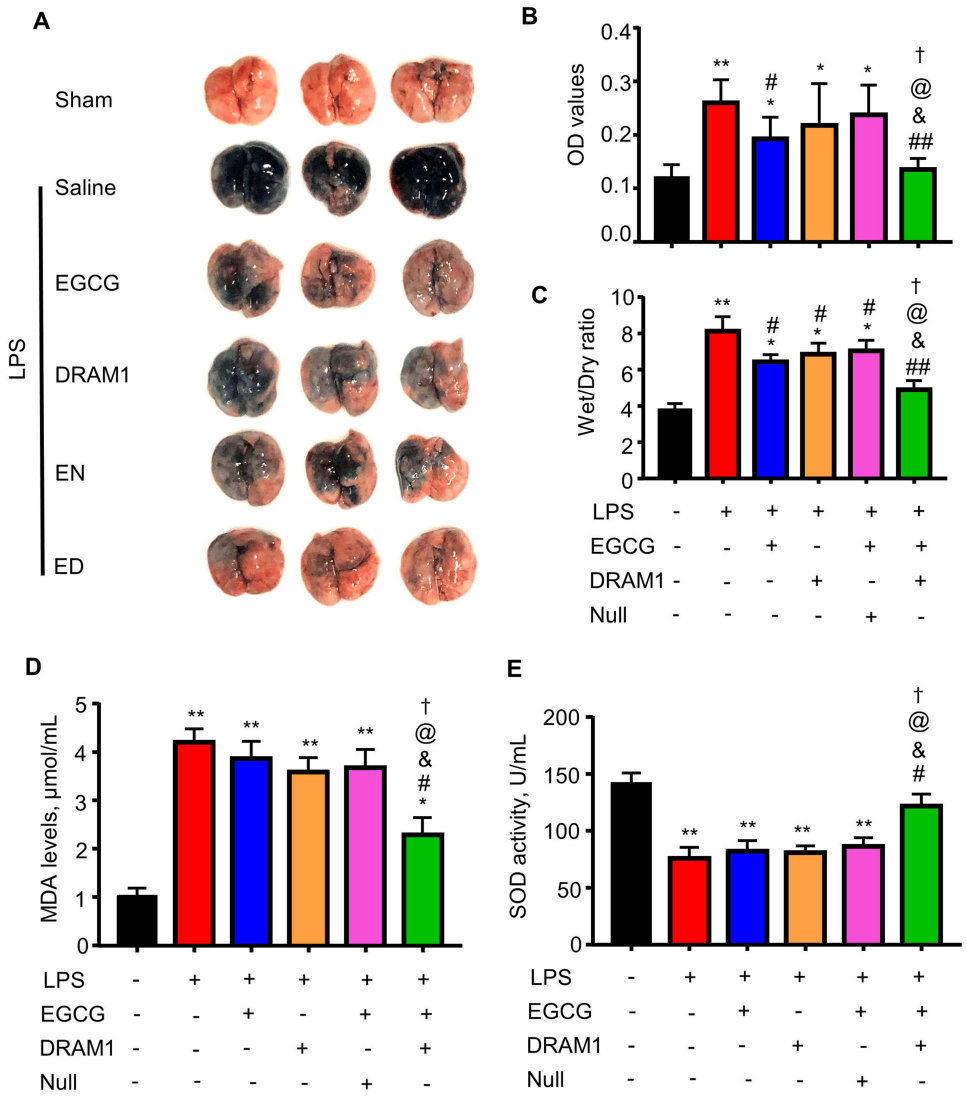

Figure 8 The effects of ED on lung vascular permeability, wet-to-dry weight ratio and oxidative stress. (**A**) Representative images of the lungs after EB staining. (**B**) Quantification of EB content in the lungs. (**C**)The wet-to-dry weight ratio (W/D weight ratio) of lung tissues from different treatment groups. (**D**) The MDA levels in lung tissues from different treatment groups. (**E**) The SOD activity in lung tissues from different treatment groups. $^{*}P < 0.05$, $^{**}P < 0.01$ vs Sham, $^{\#}P < 0.05$, $^{\#\#}P < 0.01$ vs Saline, $^{\&}P < 0.05$ vs EGCG, $^{@}P < 0.05$ vs DRAM1, $^{\dagger}P < 0.05$ vs EN.

fusion of lysosomes with autophagosomes, hence enhancing autophagy flux.[7,8] To further investigate the underlying mechanism of EGCG/DRAM1 nanoparticles on enhancing autophagy flux, we used immunoprecipitation assay to verify the relationship between Atg7 and DRAM1. The results of immunoprecipitation indicated that DRAM1 interacted with Atg7 in MLE12 cells (Figure 9F).

These results indicated that the treatment with EGCG/DRAM1 nanoparticles reduced the lung dysfunction and pulmonary edema, and promoted autophagy in the ALI mice, implying that EGCG/DRAM1 nanoparticles showed great therapeutic potential in the recovery of inflammation-induced injury lung.

Discussion

Pulmonary edema is the main pathophysiological process after ALI, which can lead to ARDS.[1,2] High-permeability pulmonary edema after ALI is still the main cause of morbidity and mortality and is a bottleneck problem in the clinical treatment of ALI.[37] Reducing pulmonary edema and oxidative stress damage is the key to improve the prognosis of ALI patients. At present, the main therapeutic strategies are auxiliary mechanical ventilation, glucocorticoid therapy and other symptomatic

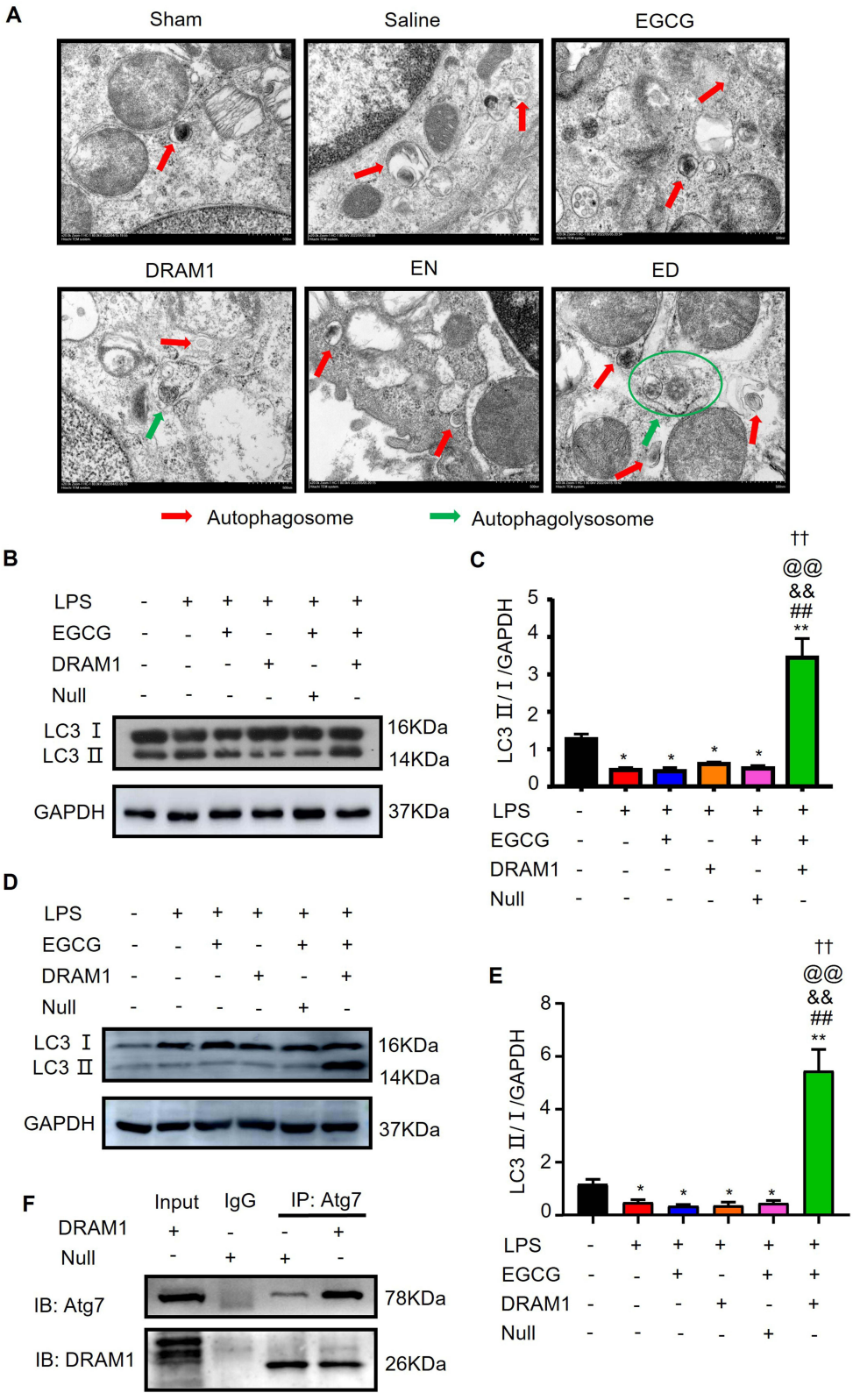

Figure 9 The effects of ED on autophagy. (**A**) The representative image of electron microscopic analysis of lung tissues from different treatment group. The red arrows indicated autophagosomes and the green arrows indicated autophagolysosomes. (**B** and **C**) The representation image and analysis results of LC3 I and LC3 II in the lung tissues. (**D** and **E**) The representation image and analysis results of LC3 I and LC3 II in MLE12 cells. (**F**) The representative image of immunoprecipitation showing interaction between DRAM1 and Atg7 in MLE12 cells. Normal IgG was used as negative control. $^{*}P < 0.05$, $^{**}P < 0.01$ vs Sham or CTL, $^{\#\#}P < 0.01$ vs Saline or PBS, $^{\&\&}P < 0.01$ vs EGCG, $^{@@}P < 0.01$ vs DRAM1, $^{\dagger\dagger}P < 0.01$ vs EN.

supportive treatment, the therapeutic effect of which is limited by undesirable side effects. Therefore, it is urgent to find a novel treatment strategy for this pathological condition. In this work, we developed a naked gene delivery system to overexpress DRAM1 for autophagy enhancement to treat ALI using EGCG, which has been shown to ameliorate oxidative stress. Mice treated with EGCG/DRAM1 nanoparticles showed ameliorated lung dysfunction as indicated by significantly increased Cdyn, PEF, MMF while reduced RAW level than EGCG, DRAM1 plasmid, EGCG/Null nanoparticles group. This is associated with reduced lung injury score, pulmonary edema and oxidative stress after EGCG/DRAM1 nanoparticles treatment.

In the current gene delivery system, EGCG was assembled with DRAM1 plasmid by forming naked nanoparticles. This nanosystem increased the stability of DRAM1 plasmid, possibly due to the negative charged surfaces of nanoparticles that are resistant to serum components. EGCG/DRAM1 nanoparticles were taken up by MLE12 cells with high efficiency and escaped from lysosome after uptake, and eventually increased DRAM1 expression effectively with no obvious cytotoxicity. Moreover, the biodistribution assay in vivo indicated that mice treated with EGCG/DRAM1 nanoparticles showed better distribution in the lung than mice treated with naked DRAM1 plasmid. This is consistent with a previous report from Wan et al showing that EGCG increased siRNA delivery efficiency with minimal toxicity in vitro and in vivo.[23]

In the development of ALI, in addition to direct injury, there are secondary pathological changes surrounding the injured tissue, including oxidative stress damage, inflammatory reaction, autophagy, and cell apoptosis.[2,13] Lee et al found that LC3B knock out mice are more susceptible to hypoxia induced pulmonary injury with reduced hypoxic cell proliferation.[38] Autophagy activation using rapamycin or RAB26 attenuates lung injury.[39,40] In addition, autophagy enhancement could reduce chemokine CXCL16 release and further improve LPS-induced ALI in mice.[41] EGCG/DRAM1 nanoparticle treated mice showed more autophagosomes and autolysosomes in lung tissues, possibly due to accelerated autophagy flux by DRAM1 and Atg7 interaction as previously described.[8] In addition, EGCG/DRAM1 nanoparticles reduced MDA levels, while increased SOD activity compared with EGCG, DRAM1 plasmid and EN group, indicating the synergistic effect of EGCG and DRAM1 overexpression on oxidative stress. ALI results in excessive generation of reactive oxygen species (ROS), leading to oxidative stress and the associated oxidative damage of cellular components, which could be inhibited by autophagy.[42] These results indicated that the therapeutic effects of EGCG/DRAM1 nanoparticles on ALI may due to the combination of autophagy activation and amelioration of oxidative stress.

Conclusion

In the current work, we developed a naked gene delivery system by EGCG to overexpress DRAM1. The synthesized EGCG/DRAM1 nanoparticles increased the stability of DRAM1 plasmid, with tolerable cellular toxicity in MLE12 cells and facilitated the accumulation and retention of DRAM1 plasmid in the infected lungs, thereby ameliorating pulmonary dysfunction after ALI. EGCG/DRAM1 nanoparticles attenuated ALI by the two mechanisms including autophagy enhancement by promoting the interaction of DRAM1 with Atg7 to increase autophagosomes, and suppression of oxidative stress by EGCG in EGCG/DRAM1 nanoparticles. Overall, the naked gene delivery system for autophagy enhancement may serve as a potential therapeutic strategy to attenuate ALI.

Acknowledgments

We would like to thank the staff of the laboratory for their help with this project.

Author Contributions

All authors contributed to data analysis, drafting or revising the article, have agreed on the journal to which the article will be submitted, gave final approval for the version to be published, and agree to be accountable for all aspects of the work.

Funding

This study was supported by the National Key Research and Development Program of China (2022YFE0209700), National Natural Science Foundation of China (82300019, 82072047, 81700382), Natural Science Foundation of Guangdong Province (2019A1515012166), Research Foundation of Education Bureau of Guangdong Province (2021ZDZX2004), Basic and Applied Basic Research Project of Guangzhou (02080390), and by the Outstanding Youth Development Program of Guangzhou Medical University. In addition, this study was supported by the Medical

Science and Technology Research Fund of Guangdong Province (A2023252). This study was also supported by the Science and technology planning project of Guangzhou (2023A04J0564). Schematic illustrations were created with BioRender.com under an academic lab subscription.

Disclosure

The authors report no conflicts of interest in this work.

References

1. Mowery NT, Terzian WTH, Nelson AC. Acute lung injury. *Curr Probl Surg*. 2020;57(5):100777. doi:10.1016/j.cpsurg.2020.100777
2. Mokra D. Acute lung injury - from pathophysiology to treatment. *Physiol Res*. 2020;69(Suppl 3):S353–S366. doi:10.33549/physiolres.934602
3. Yoshihiro S, Hongo T, Ohki S, et al. Steroid treatment in patients with acute respiratory distress syndrome: a systematic review and network meta-analysis. *J Anesth*. 2022;36(1):107–121. doi:10.1007/s00540-021-03016-5
4. YT MN, Levine B, Levine B. Methods in mammalian autophagy research. *Cell*. 2010;140(3):313–326. doi:10.1016/j.cell.2010.01.028
5. Levine B, Kroemer G. Biological functions of autophagy genes: a disease perspective. *Cell*. 2019;176(1–2):11–42. doi:10.1016/j.cell.2018.09.048
6. Qu L, Chen C, Chen Y, et al. High-mobility group box 1 (HMGB1) and autophagy in acute lung injury (ALI): a Review. *Med Sci Monit*. 2019;25:1828–1837. doi:10.12659/MSM.912867
7. Hu Y, Liu J, Wu YF, et al. mTOR and autophagy in regulation of acute lung injury: a review and perspective. *Microbes Infect*. 2014;16(9):727–734. doi:10.1016/j.micinf.2014.07.005
8. Liao SX, Sun PP, Gu YH, Rao XM, Zhang LY, Ou-Yang Y. Autophagy and pulmonary disease. *Ther Adv Respir Dis*. 2019;13:1753466619890538. doi:10.1177/1753466619890538
9. Zhang D, Li C, Zhou J, et al. Autophagy protects against ischemia/reperfusion-induced lung injury through alleviating blood-air barrier damage. *J Heart Lung Transplant*. 2015;34(5):746–755. doi:10.1016/j.healun.2014.12.008
10. Fan T, Huang Z, Wang W, et al. Proteasome inhibition promotes autophagy and protects from endoplasmic reticulum stress in rat alveolar macrophages exposed to hypoxia-reoxygenation injury. *J Cell Physiol*. 2018;233(10):6748–6758. doi:10.1002/jcp.26516
11. Zeng M, Sang W, Chen S, et al. 4-PBA inhibits LPS-induced inflammation through regulating ER stress and autophagy in acute lung injury models. *Toxicol Lett*. 2017;271:26–37. doi:10.1016/j.toxlet.2017.02.023
12. Crighton D, Wilkinson S, O'Prey J, et al. DRAM, a p53-induced modulator of autophagy, is critical for apoptosis. *Cell*. 2006;126(1):121–134. doi:10.1016/j.cell.2006.05.034
13. Guan JJ, Zhang XD, Sun W, Qi L, Wu JC, Qin ZH. DRAM1 regulates apoptosis through increasing protein levels and lysosomal localization of BAX. *Cell Death Dis*. 2015;6(1):e1624 doi:10.1038/cddis.2014.546
14. Lu T, Zhu Z, Wu J, et al. DRAM1 regulates autophagy and cell proliferation via inhibition of the phosphoinositide 3-kinase-Akt-mTOR-ribosomal protein S6 pathway. *Cell Commun Signal*. 2019;17(1):28. doi:10.1186/s12964-019-0341-7
15. Nagata M, Arakawa S, Yamaguchi H, et al. Dram1 regulates DNA damage-induced alternative autophagy. *Cell Stress*. 2018;2(3):55–65. doi:10.15698/cst2018.03.127
16. Wu X, Qin Y, Zhu X, et al. Increased expression of DRAM1 confers myocardial protection against ischemia via restoring autophagy flux. *J Mol Cell Cardiol*. 2018;124:70–82. doi:10.1016/j.yjmcc.2018.08.018
17. Alam M, Ali S, Ashraf GM, Bilgrami AL, Yadav DK, Hassan MI. Epigallocatechin 3-gallate: from green tea to cancer therapeutics. *Food Chem*. 2022;379:132135. doi:10.1016/j.foodchem.2022.132135
18. Almatroodi SA, Almatroudi A, Khan AA, Alhumaydhi FA, Alsahli MA, Rahmani AH. Potential therapeutic targets of epigallocatechin gallate (EGCG), the most abundant catechin in green tea, and its role in the therapy of various types of cancer. *Molecules*. 2020;25(14):3146. doi:10.3390/molecules25143146
19. Sharma A, Vaghasiya K, Ray E, et al. Targeted pulmonary delivery of the green tea polyphenol epigallocatechin gallate controls the growth of mycobacterium tuberculosis by enhancing the autophagy and suppressing bacterial burden. *ACS Biomater Eng*. 2020;6(7):4126–4140. doi:10.1021/acsbiomaterials.0c00823
20. Yuan C-TH C-H, Lee C-F, Chiang N-N, et al. Epigallocatechin gallate sensitizes cisplatin-resistant oral cancer CAR cell apoptosis and autophagy through stimulating AKT_STAT3 pathway and suppressing multidrug resistance 1 signaling. *Environ Toxicol*. 2017;32(3):845–855. doi:10.1002/tox.22284
21. Lee T, Oh Y, Kim MK, et al. Green tea catechol (-)-epigallocatechin gallate (EGCG) conjugated with phenylalanine shows enhanced autophagy stimulating activity in human aortic endothelial cells. *Planta med*. 2023;89(4):423–432. doi:10.1055/a-1948-4290
22. Janle EM, Morre DM, Morre DJ, et al. Pharmacokinetics of green tea catechins in extract and sustained-release preparations. *J Diet Suppl*. 2008;5(3):248–263. doi:10.1080/19390210802414279
23. Shen W, Wang Q, Shen Y, et al. Green tea catechin dramatically promotes RNAi mediated by low-molecular-weight polymers. *ACS Cent Sci*. 2018;4(10):1326–1333. doi:10.1021/acscentsci.8b00363
24. Liang K, Bae KH, Lee F, et al. Self-assembled ternary complexes stabilized with hyaluronic acid-green tea catechin conjugates for targeted gene delivery. *J Control Release*. 2016;226:205–216. doi:10.1016/j.jconrel.2016.02.004
25. Chung JE, Tan S, Gao SJ, et al. Self-assembled micellar nanocomplexes comprising green tea catechin derivatives and protein drugs for cancer therapy. *Nat Nanotechnol*. 2014;9(11):907–912. doi:10.1038/nnano.2014.208
26. Yang HH, Duan JX, Liu SK, et al. A COX-2/sEH dual inhibitor PTUPB alleviates lipopolysaccharide-induced acute lung injury in mice by inhibiting NLRP3 inflammasome activation. *Theranostics*. 2020;10(11):4749–4761. doi:10.7150/thno.43108
27. Hu Y, Lou J, Mao YY, et al. Activation of MTOR in pulmonary epithelium promotes LPS-induced acute lung injury. *Autophagy*. 2016;12(12):2286–2299. doi:10.1080/15548627.2016.1230584
28. Zhou J, Peng Z, Wang J. Trelagliptin alleviates lipopolysaccharide (LPS)-induced inflammation and oxidative stress in acute lung injury mice. *Inflammation*. 2021;44(4):1507–1517. doi:10.1007/s10753-021-01435-w

29. Zhu Y, Han Q, Wang L, et al. Jinhua Qinggan granules attenuates acute lung injury by promotion of neutrophil apoptosis and inhibition of TLR4/MyD88/NF-κB pathway. *J Ethnopharmacol*. 2023;301:115763. doi:10.1016/j.jep.2022.115763
30. Qin YY, Huang XR, Zhang J, et al. Neuropeptide Y attenuates cardiac remodeling and deterioration of function following myocardial infarction. *Molecular Ther*. 2022;30(2):881–897. doi:10.1016/j.ymthe.2021.10.005
31. Wang D, Wang X, Tong W, et al. Umbelliferone alleviates lipopolysaccharide-induced inflammatory responses in acute lung injury by down-regulating TLR4/MyD88/NF-kappaB signaling. *Inflammation*. 2019;42(2):440–448. doi:10.1007/s10753-018-00953-4
32. Park J, Chen Y, Zheng M, et al. Pterostilbene 4-β-glucoside attenuates LPS-induced acute lung injury via induction of heme oxygenase-1. *Oxid Med Cell Longev*. 2018;2018:2747018. doi:10.1155/2018/2747018
33. Cheng HT, Yen CJ, Chang CC, et al. Ferritin heavy chain mediates the protective effect of heme oxygenase-1 against oxidative stress. *Biochim Biophys Acta*. 2015;1850(12):2506–2517. doi:10.1016/j.bbagen.2015.09.018
34. Wu X, He L, Chen F, et al. Impaired autophagy contributes to adverse cardiac remodeling in acute myocardial infarction. *PLoS One*. 2014;9(11):e112891. doi:10.1371/journal.pone.0112891
35. Meng J, Qin Y, Chen J, et al. Treatment of hypertensive heart disease by targeting smad3 signaling in mice. *Mol Ther Meth Clin Develop*. 2020;18:791–802. doi:10.1016/j.omtm.2020.08.003
36. Liu B, Zhao H, Wang Y, et al. Astragaloside IV attenuates lipopolysaccharides-induced pulmonary epithelial cell injury through inhibiting autophagy. *Pharmacology*. 2020;105(1–2):90–101. doi:10.1159/000502865
37. Bhargava M, Wendt CH. Biomarkers in acute lung injury. *Transl Res*. 2012;159(4):205–217. doi:10.1016/j.trsl.2012.01.007
38. Lee SJ, Smith A, Guo L, et al. Autophagic protein LC3B confers resistance against hypoxia-induced pulmonary hypertension. *Am J Respir Crit Care Med*. 2011;183(5):649–658. doi:10.1164/rccm.201005-0746OC
39. Zhao H, Chen H, Xiaoyin M, et al. Autophagy activation improves lung injury and inflammation in sepsis. *Inflammation*. 2019;42(2):426–439. doi:10.1007/s10753-018-00952-5
40. Dong W, He B, Qian H, et al. RAB26-dependent autophagy protects adherens junctional integrity in acute lung injury. *Autophagy*. 2018;14(10):1677–1692. doi:10.1080/15548627.2018.1476811
41. Gao Y, Wang N, Li RH, et al. The role of autophagy and the chemokine (C-X-C motif) ligand 16 during acute lung injury in mice. *Med Sci Monit*. 2018;24:2404–2412. doi:10.12659/MSM.906016
42. Ornatowski W, Lu Q, Yegambaram M, et al. Complex interplay between autophagy and oxidative stress in the development of pulmonary disease. *Redox Biol*. 2020;36:101679. doi:10.1016/j.redox.2020.101679